Dist: A

REPORT DOCUMENTATION PAGE

Form Approved
OMB No. 0704-0188

1. AGENCY USE ONLY (Leave blank)	2. REPORT DATE	3. REPORT TYPE AND DATES COVERED
	10 Feb 95	Final, 14 Jun 94-14 Dec 94

4. TITLE AND SUBTITLE
mm-wave resonant methods for the detection of corrosion

5. FUNDING NUMBERS
C
F49620-94-C-0049
6550QF
3005/SS

6. AUTHOR(S)
J. Martens and S. Sachtjen

7. PERFORMING ORGANIZATION NAME(S) AND ADDRESS(ES)
Conductus, Inc.
969 West Maude Avenue
Sunnyvale, CA 94086

8. PERFORMING ORGANIZATION REPORT NUMBER
95-C-SRA-001
AFOSR-TR-95-0099

9. SPONSORING/MONITORING AGENCY NAME(S) AND ADDRESS(ES)
AFOSR/NL
110 Duncan Avenue
Suite B115
Bolling AFB, DC 20331-0001
Maj Thomas E. Erstfeld

10. SPONSORING/MONITORING AGENCY REPORT NUMBER

11. SUPPLEMENTARY NOTES

12a. DISTRIBUTION/AVAILABILITY STATEMENT
Unlimited

12b. DISTRIBUTION CODE
A

13. ABSTRACT *(Maximum 200 words)*

In this program, a class of mm-wave resonant tools known as surface resistance analyzers were evaluated for their ability to detect corrosion and extract information on corrosion products. The study was performed primarily on aluminum alloys exposed to salt fog conditionsalthough a high temperature materialsand steel alloys were also measured. The results on detection were uniformly encouraging. Statistically significant deviations in surface resistance were reported prior to visible corrosion products appearing. Incipient stress-related cracks around rivet holes were also detected on length scales of 0.1 mm. Complex permittivity data was extracted for the corrosion products and was used to estimated thicknesses, impurity levels, and composition changes during different expsoure conditions. Incipient corrosion was also detected underneath several varieties of paint. The results suggest that this may be a useful measurement tool for the detection and analysis of corrosion in an aircraft maintenance environment.

14. SUBJECT TERMS	15. NUMBER OF PAGES
NDE, corrosion detection, mm-wave analysis resonant analysis	37
	16. PRICE CODE

17. SECURITY CLASSIFICATION OF REPORT	18. SECURITY CLASSIFICATION OF THIS PAGE	19. SECURITY CLASSIFICATION OF ABSTRACT	20. LIMITATION OF ABSTRACT
Unclassified	Unclassified	Unclassified	UL

Air Force Office of Scientific Research
Final Technical Report
February 1995

MM-WAVE RESONANT METHODS FOR THE DETECTION OF CORROSION

F49620-94-C-0049

Conductus, Inc.

J. Martens and S. Sachtjen

AIR FORCE OFFICE OF SCIENTIFIC RESEARCH
BOLLING AFB, DC 20332

TABLE OF CONTENTS

PHASE I FINAL REPORT

CONTRACT F49620-94-C-0049

MM-WAVE RESONANT METHODS FOR THE DETECTION OF CORROSION

Executive Summary

In this program, a class of mm-wave resonant tools known as surface resistance analyzers were evaluated for their ability to detect corrosion and extract information on corrosion products. The study was performed primarily on aluminum coupons (and modifications thereof) exposed to salt fog conditions although several high temperature alloys and painted coupons were also measured. The results on detection were uniformly encouraging. Statistically significant deviations in surface resistance were reported prior to visible corrosion that was later corroborated microscopically. Incipient stress-related cracks around rivet holes were also detected on length scales of 100 μm. Complex permittivity data were extracted for the corrosion products and were used to estimate thicknesses, impurity levels and composition changes during different exposures. Incipient corrosion was also detected underneath several varieties of paint and on high temperature alloys. The results suggest that this may be a useful measurement tool for the detection and analysis of corrosion in an aircraft maintenance environment.

1 Objectives

A sequence of experiments and measurements were designed to evaluate the mm-wave tools in their ability to detect and analyze corrosion products. Of obvious interest are aircraft-relevant materials and these were used throughout. A salt-fog environment was used for most samples except the high temperature alloy and a variety of exposure times were used. To meet the evaluation goals, the following objectives were used:

1. Algorithmic automation and minor hardware improvements to improve the extraction of complex permittivity of the samples and corrosion products.

2. Generation of test samples of aluminum and steel coupons (and possible composites samples), riveted metals, stressed and/or painted samples. This will be done both at Conductus and at the subcontractor, Sandia National Laboratories.

3. Detection of corrosion tests. Compare signatures of microscopic, microbalance and resonant measurements to determine the sensitivity of the resonant technique and to correlate measurements with macroscopic structural parameters. This will be done on the samples generated in step 2.

4. Analysis of corrosion products. Use the complex permittivity extracted from the resonant analysis to evaluate the kinetics in the corroded samples. The extracted thickness and composition data should be able to determine the geometric structures most likely to corrode and which corrosion components are responsible. This could then be used to suggest coatings or other treatment scenarios.

5. Analyze corrosion growth products as a function of surface pretreatment or other conditions.

2 Technical Problem

As military and commercial aircraft fleets age, the importance of early corrosion detection increases. One reason is that, in the current economic environment, revenue streams do not exist to replace aircraft as often as in the past. Many military and other aircraft are now being required to stay in service for decades beyond their original design life, e.g.,

KC135 to be in service until 2040
C141 to be in service until 2040
737s expected to be used until 2030

Corrosion repair expenditures for aircraft are already over 1 billion dollars per year. Proper diagnostics of aircraft structures will enable the detection of problems before macroscopic structural damage occurs. The economic and safety implications of better detection methods are enormous, as evidenced by the billions of dollars in resources that the FAA and the Air Force have put forth already.

Tools (and, more globally, techniques) capable of detecting corrosion early and extracting information about the corrosion are extremely important in containing costs, improving repair times and reducing the probabilities of catastrophic failure prior to detection/repair. The ideal tool will be non-contact, sensitive to nascent corrosion, be able to provide some information on the corrosion product that may lead to its cause or enhancing factors, and amenable to field use. The tool should ideally also be able to detect corrosion problems in one of the more critical areas: near rivet holes. Many existing techniques fail in one or more of these respects. A newer technique, based on the use of mm-wave resonant analysis offers some hope of meeting more of these criteria for a useful tool. The measurement is based on forming a quasi-optical cavity between the aircraft or other part and the measurement system. The structure as described in the proposal is shown in Fig. 1.

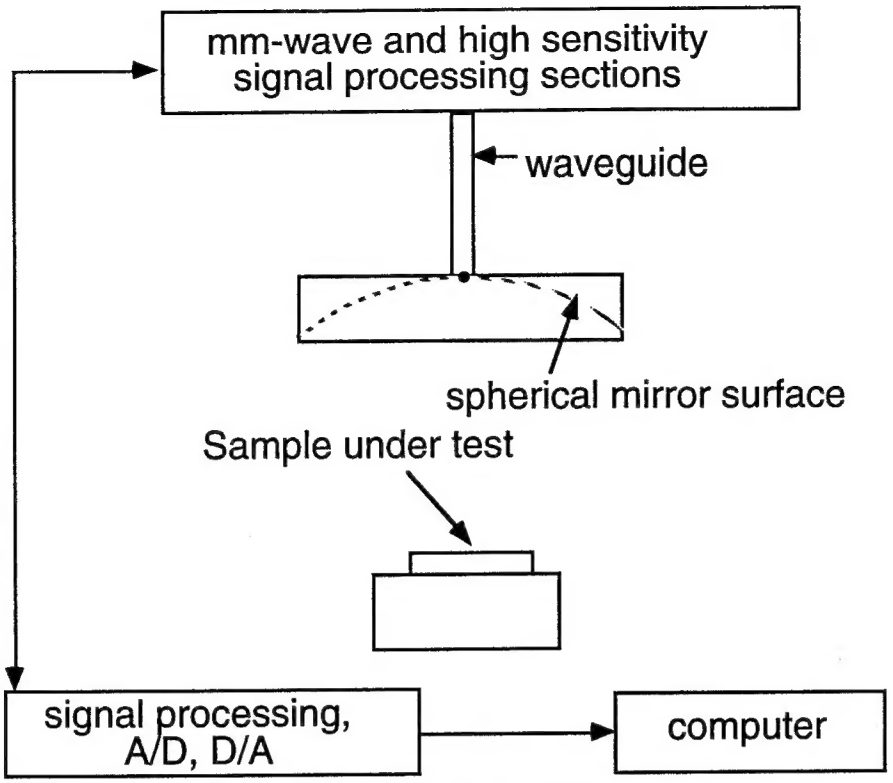

Figure 1. *Basic structure of the mm-wave test system known generically as a surface resistance analyzer.*

An electromagnetic wave bounces between the spherical mirror and the quasi-planar sample under test. Any losses on the sample will affect the amount of energy reflected within the cavity, and hence the measured values of resonator quality factor (Q) and resonant frequency. Most corrosion products can be characterized as lossy dielectrics hence their presence on the surface will increase power lost in the cavity. Small cracks on or near the surface of the metal will disrupt rf current flow on the metal and will hence also increase local loss. Thus both of the major corrosion events will increase power lost within the cavity and therefore, the measured surface resistances will increase. This is the prime mode of corrosion detection with this approach. Variations in resonant frequency and in surface resistance with frequency can allow the extraction of additional information such as purity of the corrosion product and some compositional information.

The object of this program was to see if these measures of corrosion are sufficiently sensitive and accurate to be useful for an aging aircraft environment. The

measurements discussed above were used on a variety of samples (exposed to a variety of conditions) to determine the ability to detect corrosion and what kinds of information were extractable.

3 Methodology

As discussed in section 2, this program is focused on evaluating the applicability of mm-wave resonant techniques for the detection and analysis of corrosion products. The basic instrument, shown in Fig. 1, was used for the bulk of the measurements at an operating frequency near 94 GHz. A multi-frequency variant was used for a few exploratory measurements and will be discussed later.

A spherical mirror and the sample under test form the two ends of the resonant cavity. In the measurement, two quantities are directly measured: the quality factor Q and the resonant frequency f_0. The quality factor is inversely related to the width of the resonance and reduces when the losses become larger (either from substrate resistivity increasing or dielectric loss increasing). The meaning of the resonant frequency is clear from the previous discussion on the box resonator. From these measured quantities, the surface resistance can be extracted from a simple formula [1,2]

$$R_s = \frac{\pi f_0 \mu_0 b}{2Q} - R_{sm} \qquad (1)$$

where b is the radius of curvature of the mirror, μ_0 is the free space permeability ($4\pi\ 10^{-7}$ H/m) and R_{sm} is the mirror surface resistance in Ω. The surface resistance, R_s, is the variable used in many of the plots to follow and is a good measure of the overall loss in a composite sample. It would be the predominant variable when searching for corrosion since it unambiguously indicates a loss increase. In the case of subsurface cracks around rivets, for example, this is more useful than a precise dielectric evaluation.

In more conventional corrosion problems, dielectric information can be extracted to aid in kinetics analysis. A two-layer model (a complex dielectric on top of a conducting substrate) is generally assumed; it works well on problems studied to date and simplifies the analysis. As discussed above, the resonant frequency shifts because of the presence of a layer of different wave velocity. Thus, the difference in resonant frequency (with and without the product layer) provides information on the layer's dielectric properties and thickness. This relation is expressed as [3]

$$t \propto \frac{\Delta f_0}{\sqrt{\varepsilon_r} - 1} \qquad (2)$$

where t is the product thickness, Δf_0 is the change in resonant frequency and ε_r is the relative permittivity of the product. Similarly, the complex dielectric properties can be extracted from the change in Q (or equivalently in R_s). The complex permittivity ($\varepsilon=\varepsilon'-j\varepsilon''$) is related to the measured variable by [3]

$$\frac{\varepsilon_r''}{\varepsilon_r - 1} = \frac{f_{00}}{2(\Delta f_0)} \cdot \left(\frac{1}{Q_{01}} - \frac{1}{Q_{00}} \right) \qquad (3)$$

where ε_r'' is the relative imaginary part of permittivity, f_{00} is the base resonant frequency and Q_{01} and Q_{00} are the resonator quality factors after and before the presence of the corrosion product, respectively.

Surface resistance will be used as the standard variable in most of the discussion to follow because it is a sensitive measure of loss within a few to 10 skin depths of the surface of the sample. This is an extremely important concept in interpreting the data. The skin depth is the distance that an electromagnetic field penetrates into a material (the decay length in an exponential sense) and is dependent on the resistivity of the material and the frequency. For materials dominated by single electron conduction (all metals and most corrosion products), the skin depth δ can be defined by [3]

$$\delta = \sqrt{\frac{\rho}{\pi f_0 \mu_0}} \qquad (4)$$

where f_0 is the test frequency and ρ is the material resistivity. A very pure oxide (on Si for example) is one example where this equation is not valid but in that case the field penetration is indeed very large. For common aluminum alloys (1100,2024, 6061, 7075) at the standard test frequencies near 94 GHz, the skin depth will be in the range of 0.25-0.45 μm. Thus IN THE BULK ALUMINUM, the measurements will be dominated by the top few μm of material [4]. The resistivities in corrosion products are much higher making the skin depth in those materials much larger, typically many hundreds of μm. Thus in a typical measurement, all of the corrosion product and part of the metal surface will be sampled. In the case of corrosion cracking, obviously any products in this range will be detected as will any cracks relatively near the surface. To see how this works, consider what happens on an electronic level when the mm-wave beam hits the surface. To match boundary conditions on the metal surface, an rf current must be set up in the metal (depth into the metal of about a skin depth) and flows in a pattern roughly matching that of the incident field. It is this current that generates the reflected wave. Any energy dissipated by this current will reduce the reflected energy and hence increase the measured surface resistance. If the current is forced to deviate because of a crack near the surface (or other obstructions such as large grain inclusions), its energy loss must increase if for path length reasons if nothing else. Thus a crack or other defect will cause an elevated surface resistance reading.

The basic measurement concepts discussed above have been implemented in a commercial product for the analysis of metallizations, semiconductors and dielectrics. The modifications for this work are primarily in simplifying the extraction of complex permittivity (making that portion directly dual-use) and setting up for some simple multi-frequency measurements. The remainder of the work in the program is the measurement and analysis of a variety of technologically interesting samples for corrosion detection and extraction of product information. Since many of these results are applicable to corrosion problems outside of military airframes, the rest of the work can also be constituted as dual-use.

4 Technical results

The work described in section 1 can be broken down into three main groups: 4.1: setup and algorithmic changes, 4.2: sample generation and testing, 4.3: sample testing under ancillary conditions. The results are separated accordingly.

4.1 Algorithmic automation

The purpose of this initial phase was to set up for the later measurements by automating extraction of complex permittivity data and to allow for some limited multi-frequency analysis should it be necessary. For the standard complex permittivity extraction, a fairly simple variational model was used resulting in an algorithmic form of Eq. 3. This approach is valid as long as the layer of interest is not more than about a skin depth thick. As discussed above, this limits product thickness to several hundred μm. Such thick products obviously are not of interest as a detection problem and are probably sufficiently stratified that a permittivity extraction would be extremely difficult. As is obvious from the equations, reference resonant frequency and Q are required which correspond to the base metallization. For these simple experiments, coupons of the appropriate alloys prior to exposure were available for measurement. Local means on these unexposed (cleaned prior to measurement but with a thin oxide present) were used for the references. Because of the initial oxide presence, there may be an error in thickness of 1-10 nm on these samples. Based on the corrosion products encountered, this should not be an issue.

The analysis was used to successfully characterize SiO_2 layers, other microelectronic dielectrics and several polymer coatings (including photoresists and polyimides) during qualification. For the range of conditions expected for corrosion products, the accuracy on loss tangent was generally better than 10%.

Multifrequency analysis was another algorithm set explored. While a single frequency measurement can extract two out of the three parameters t, ε', ε''; it would sometimes be useful to simultaneously extract all three. Since a single frequency measurement only produces two quantities (f and Q or alternatively real and imaginary parts of surface impedance), this would seem difficult. Recall the concept of skin depth where the probing field depth varies with frequency. Measurements at different frequencies would then be sampling a different mix of product and base metal and would allow for differentiation. The effect can be seen in the following general equation [5] for surface admittance of a two layer structure as a function of frequency.

$$Y_{s,eff} = \frac{1}{\sqrt{2\omega\mu_0\sigma_1}\left[\frac{1}{2\sigma_1} + \omega\mu_0 t_2^2 + 2t_2\sqrt{\frac{\omega\mu_0}{2\sigma_1}}\right]}$$

$$\left\{\begin{array}{l}\left[1 + 2\omega t_2\varepsilon''\sqrt{\frac{\omega\mu_0}{2\sigma_1}} + \omega^2\mu_0 t_2^2(\varepsilon' + \varepsilon'')\right] + \\ j\left[-1 + 2\omega t_2\varepsilon'\sqrt{\frac{\omega\mu_0}{2\sigma_1}} + \omega^2\mu_0 t_2^2(\varepsilon' - \varepsilon'') - \omega\mu_0 t_2\sqrt{\frac{2\sigma_1}{\omega\mu_0}}\right]\end{array}\right\} \quad (5)$$

where σ_1 is the conductivity of the base metal, t_2 is the thickness of the product and ε'-$j\varepsilon''$ is the complex permittivity of the product. From the reference measurement, there are the three unknowns and a two frequency measurement would produce 4 knowns thus slightly over-specifying the problem. A simple fitting routine can then be used to extract the parameters. This technique is still being tested but shows accuracy improvements so far, particularly on thinner dielectrics where Eq. 3 runs into resolution problems.

4.2 Sample generation, detection of corrosion and analysis of products

4.2.1 First sample set: Al alloys and salt fog

The first set of samples consisted of coupons from 4 aluminum alloys (1100,2024,6061, and 7075) to be measured before and after salt fog exposure (168 hours, 3.5% solution of NaCl in water atomized). The object was to correlate the surface impedance/permittivity signatures extracted from the resonant technique with microscopic analysis and with results obtained from other techniques.

Before exposure, the surface resistances of the alloys were all reasonably consistent with what one would expect for these bulk metals with some starting surface oxide. Starting samples with varying levels of oxides affected the absolute numbers but not the relative changes to any great degree. After exposure, the surface impedance changed dramatically as indicated in the table below. Here W=windward and L=leeward refers to the side of the sample receiving and looking away from the salt fog generator respectively. The measured numbers are surface resistances in ohms.

Alloy	Before	After W	% change	After L	% change
1100	0.176	0.226	*+28%*	0.208	*+18%*
6061	0.222	0.305	*+37%*	0.266	*+20%*
7075	0.258	0.461	*+79%*	0.376	*+46%*

There is clearly a difference among the alloys in corrosion resistance, as has been confirmed by many other measurement techniques (quartz microbalance, microscopic inspection,...). The thickness of the corrosion products was extracted from resonant frequency differentials and the ratio of these thicknesses (1100 product thickness:6061 product thickness: 7075 product thickness) was about 1:2.2:4. Before and after contour

maps of the 6061 alloy are shown in Fig. 2 to illustrate the fairly dramatic nature of the surface resistance shift.

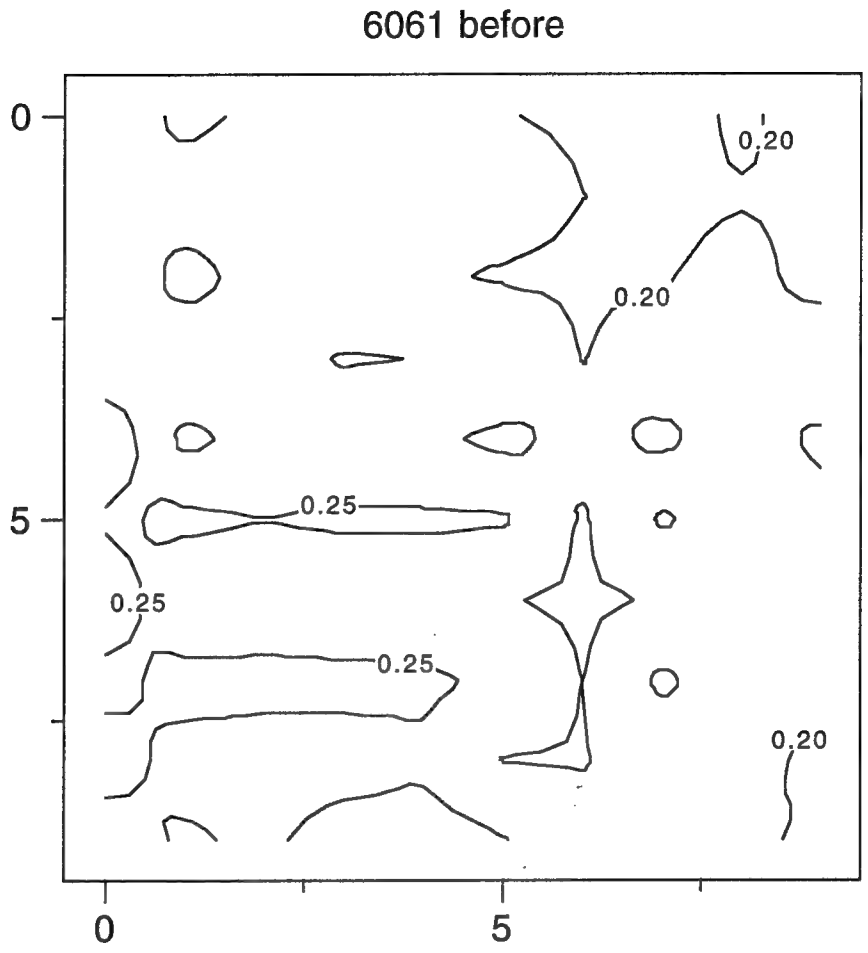

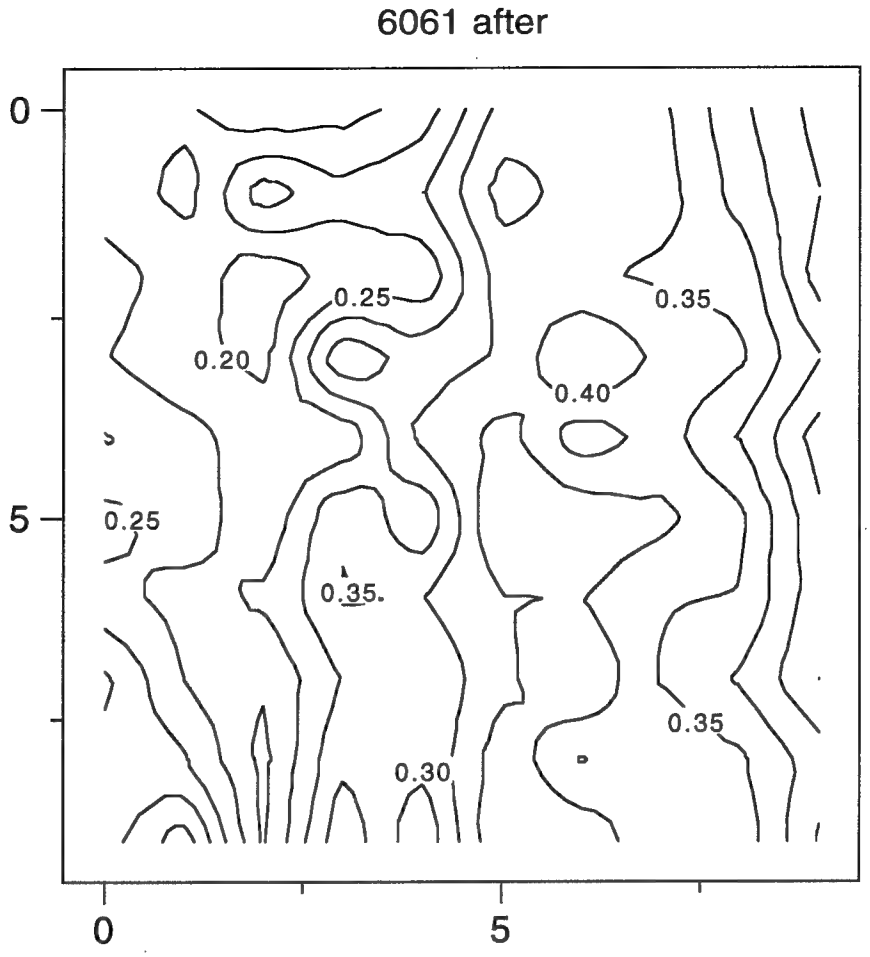

Figure 2. *Contour plots of a section of 6061 Al before and after salt fog exposure. The contour labels are surface resistances in ohms. The absolute change is obvious as is the increase in inhomogeneity. The lateral scales are 2 mm/div (full scale, the plots are 10 divisions wide).*

The loss tangent of the product layer also increases through the series of samples (by a factor of 3). Since the loss tangents are all higher than that of pure Al_2O_3, the product layers are becoming increasingly diverse chemically as one moves through the series with the 7075 product layer being dominated by contaminant oxides. This is also consistent with many microscopic observations. Also of interest is that the standard deviation of loss tangent (on a spatial basis) is about 8 times higher for the 7075 than for the 1100 suggesting a 7075 nucleation model with very different distance scales.

These observations would be consistent with nucleation centering on the denser impurity sites. Further evidence is provided by some limited multi-frequency analysis which showed the standard deviation of loss tangent decreasing away from the metal surface. The dielectric properties would be more unstable near these impurity sites and would presumably become somewhat more stable at the upper layers of the product.

4.2.2 Sample with rivet holes and other stresses

Since one of the critical corrosion problems involves subsurface cracking near rivet holes, samples to simulate this condition were generated (pending actual aircraft samples). Rivet holes were placed in a 7075 coupon (1/8" thick) that had already had salt fog exposure but was not coated with any pretreatment. The sample was then placed under bending stress while in a salt water environment (to accelerate any effects) for 24 hours. The before and after contour maps are shown in Fig. 3. Prior to the stress and exposure, the holes were clearly defined by deviations in local surface resistance. After exposure, another region of elevated surface resistance appeared around the hole areas that is asymmetric. Since the bending force was applied against the vertical edges of the image, this may be consistent with microcrack formation. A more complete analysis needs to be done of this type of test, but a change was detected around the holes that could not be detected optically.

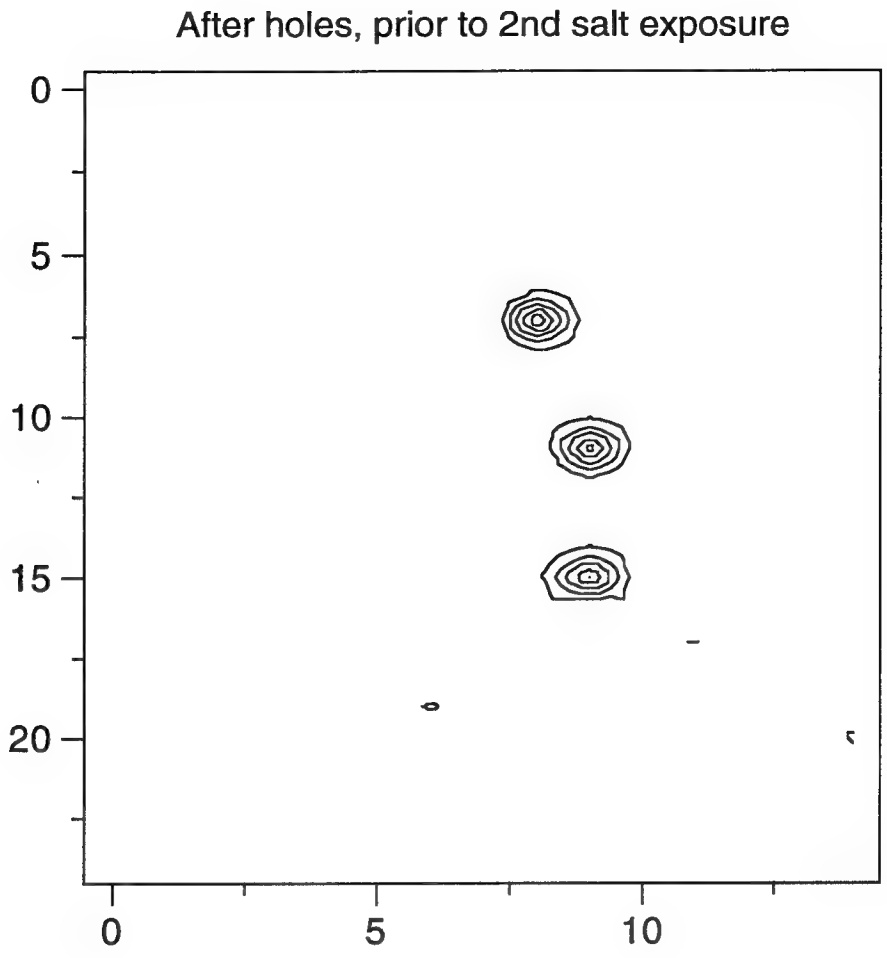
After holes, prior to 2nd salt exposure
0
5
10
15
20
0
5
10

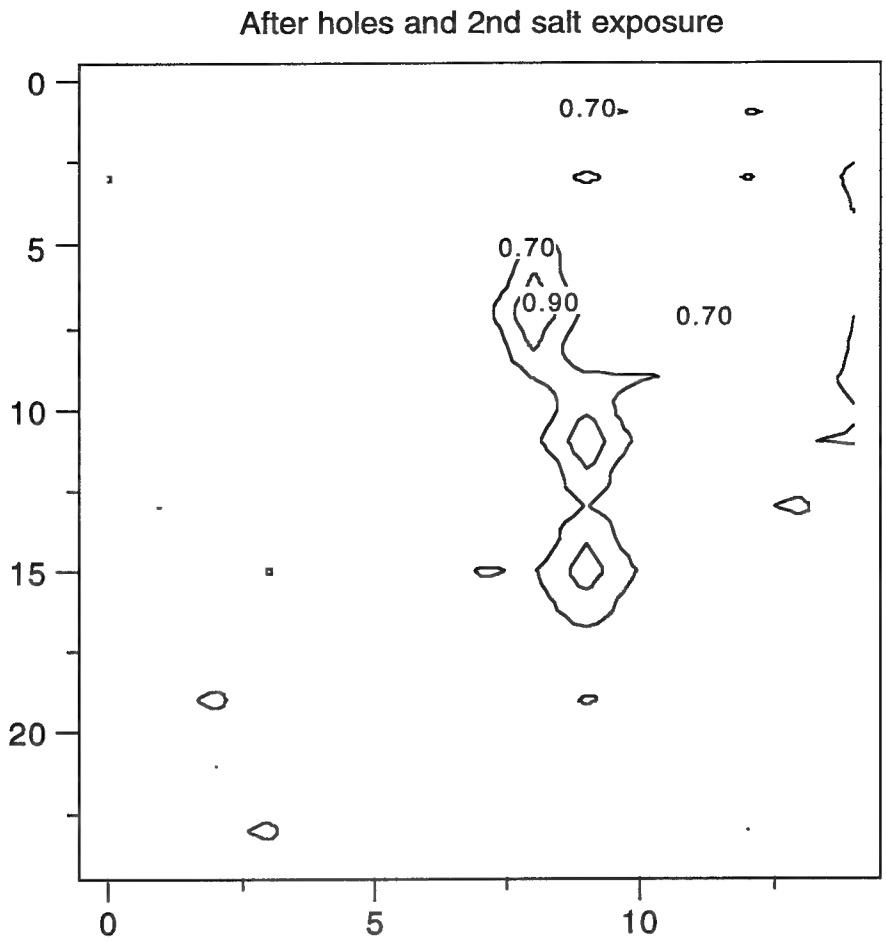

Figure 3. *Surface resistance contour plots (in ohms) of a 7075 coupon with rivet-like holes placed in it. The images are for before and after a salt exposure. Note the added elongated distortion in the surface resistance data after exposure. The contour values start at a high level to focus on the hole areas. The significant surface disruption of the corrosion on the blank metal is not shown.*

Some additional tests were conducted to try to correlate the surface resistance signature with the exposure conditions and, if possible, to the incipient crack sizes. A measure that was used was the effective area that had a surface resistance elevated at least 50% above the background mean. Since the rivet hole sizes were constant (diameter of about 5 mm), this should provide a measure of the disrupted area.

Because of time constraints, only a limited number of tests were run, but the data illustrates a clear trend. Keep in mind that the effective area includes the rivet hole itself. Small cracks were microscopically evident for the last row in the table with sizes on the order of 100 μm. This should give some estimate of the measurable effect size.

Conditions	**Effective elevated area (mm^2)**
1 day, nominal bending stress	76
2 days, nominal bending stress	81
3 days nominal bending stress	85
4 days, double bending stress	93

4.2.3 steel tests

Although not as commonly used in aircraft parts, some steels were also analyzed to give another base line measurement. Because FeO_x is a much lossier dielectric than the aluminum corrosion products (and grows much faster), this is a far easier detection problem. Figure 4 illustrates the trend for a cold rolled steel sample before and during an exposure to a 100% RH environment (salt fog). A protective oil coating was removed just prior to the original measurement. The change is quite dramatic (no visible change yet) and clearly illustrates some of the sensitivity issues involved. Assuming a dielectric constant of 12 for FeO, the thickness extracted from this measurement (at the end of the measurement cycle) is around 100 nm.

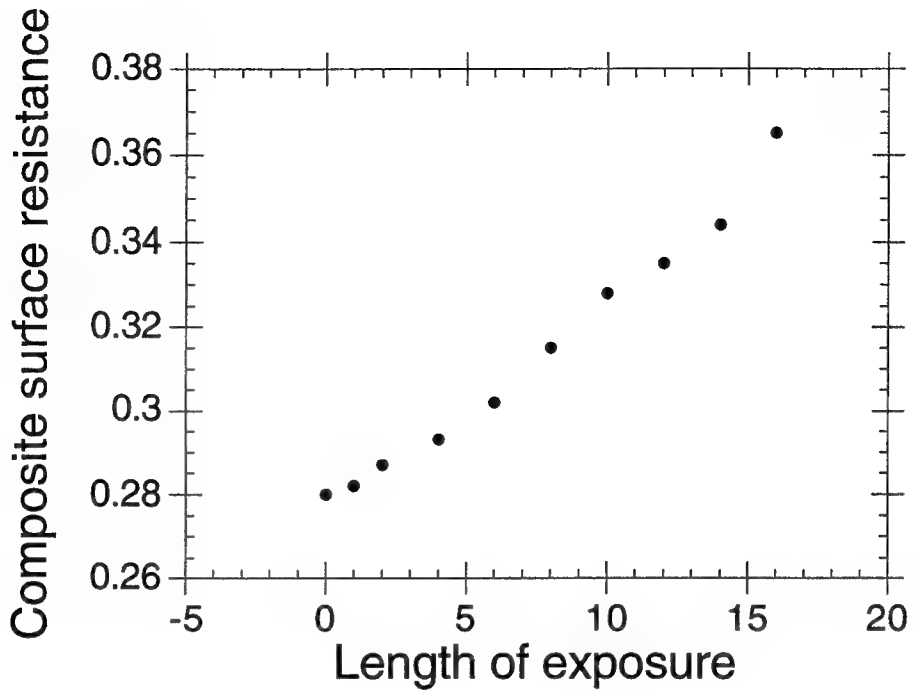

Figure 4. *Composite surface resistance of a cold rolled steel sample during exposure to a salt fog environment at elevated temperature (about 40°C). The time units are hours.*

At a few of the exposure times indicated above, both single and dual frequency measurements were performed as a preliminary test/comparison of the newer measurement technique. At exposure times of 8 and 16 hours, the dual frequency analysis produces dielectric constants of 11.9 and 11.3 respectively. These are increasingly lower than what one might naively expect. It is possible that voids are forming in the thicker coats, lowering the effective dielectric constants. Extracted thicknesses were then compared. To make the comparison as fair as possible, the extracted dielectric constants listed above were used for the single frequency thickness extraction. At an exposure time of 8 hours, the thicknesses were 45 nm from single frequency and 59 nm from the dual frequency measurement. At an exposure time of 16 hours, the values were 104 and 111 nm respectively. As might be expected, the values display greater agreement at higher thicknesses.

4.2.4 Tests underneath paint

Since in many field applications it would be desirable to detect corrosion beneath paint, it is important to determine if (a) paints are too lossy to allow this measurement and (b)what degree of sensitivity is possible. The first experiments were conducted with steel coupons painted with either epoxy or powder paints. A scratch of 1±0.2 mm width was cut in the paint and the coupons exposed to salt fog. The final coupon was then measured to see if corrosion was detectable beneath the paint. Figure 5 shows the results for two coupons measured under these circumstances. The scratch extends horizontally from x=0 index marks to about x=10 in both cases. The background surface resistance stayed in the 0.3-0.4 ohm range but the disruption near the scratch is significant. In the heavy exposure case, disruption in surface resistance is visible nearly 2 cm from the scratch. Since the spot size is certainly no larger than 5 mm, this indicates the presence of products beneath the paint surface at a significant distance from the scratch. The total disruption width is about 50 mm in the heavy case and 35 mm in the moderate case.

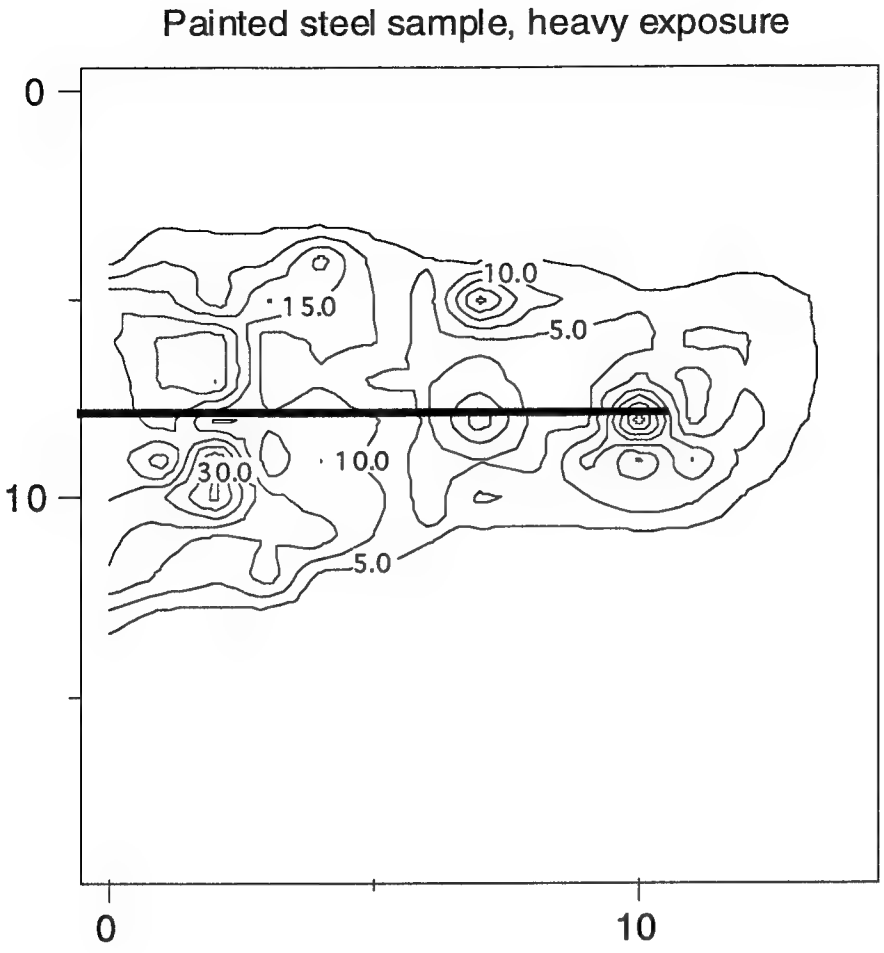
Painted steel sample, heavy exposure
0
10
0
10
15.0
10.0
5.0
30.0
10.0
5.0

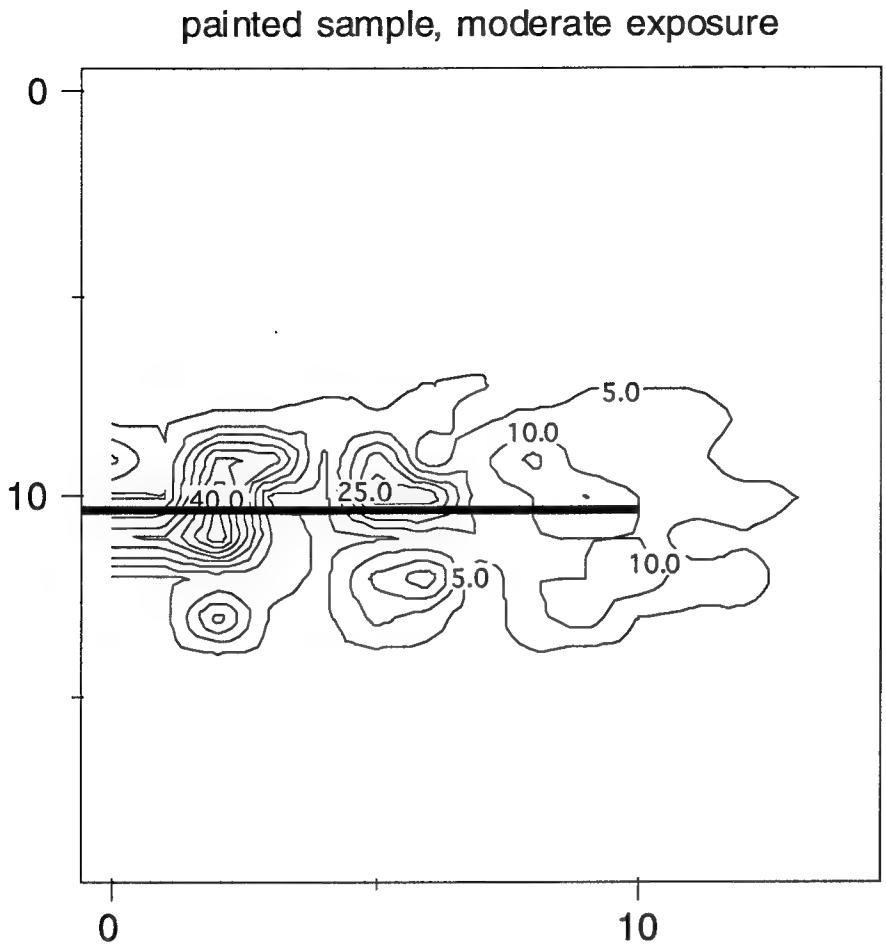

Figure 5. *Contour plot of painted steel sample (with a scratch 1 mm wide) exposed to a salt fog environment for two different durations. The lateral scales are 5 mm/div and the contour labels are surface resistances. The position of the scratch is indicated approximately by the heavy black line.*

The experiments were repeated on some aluminum samples and in no case was the paint loss a significant factor in corrosion detection. The paint clearly impedes extraction of the real part of permittivity since an additional phase delay source is present but it should be less of a problem in detectability. This ability is extremely important in field application, since bare surfaces will often not be available.

4.2.5 Salt fog matrix

To obtain a more complete understanding of the detectability limits, a matrix of Al alloys run under different salt fog and humidity conditions was performed. Three different alloys (2024, 6061 and 7075, all T6) were each exposed to four different conditions for a total of 12 samples. The virgin surface resistances were within 1% of those discussed earlier for these alloys (0.248 Ω for 2024 which was not available earlier). The salt fog conditions were based on the same 3.5% NaCl atomized solution mentioned in a previous subsection. The last 3 samples for each alloy included humidity exposure (>90% RH at 30°C) with the longest exposure being 7 days. The surface resistances presented in the below table are means from scans over 1 cm x 1 cm boxes. The 'light,' 'moderate,' and 'heavy' descriptors refer to length of exposure in the humidity chamber.

Sample	Mean surface resistance (Ω)	Change from virgin
2024 fog 3 days	0.333	+34%
2024 fog 7 days + light humidity	0.398	+60%
2024 fog 7 days + moderate humidity	0.524	+111%
2024 fog 7 days + heavy humidity	0.604	+144
6061 fog 3 days	**0.257**	**+16%**
6061 fog 7 days + light humidity	**0.283**	**+27%**
6061 fog 7 days + moderate humidity	**0.359**	**+62%**
6061 fog 7 days + heavy humidity	**0.361**	**+63%**
7075 fog 3 days	0.350	+36%
7075 fog 7 days + light humidity	0.409	+59%
7075 fog 7 days + moderate humidity s	0.522	+102%
7075 fog 7 days + heavy humidity	0.591	+129%

The trends are consistent with what one would expect from these alloys and from microscopic analysis. The 6061 seems to self-passivate towards the end of this humidity test which would suggest a purer and more uniform oxide layer. This is consistent with loss tangent analysis which placed that for 6061 among the lowest. The final loss tangent here is somewhat lower (by about 30%) than that determined just from salt fog exposure. This may be because the composition of the product is shifting during the later humidity exposures to something more closely approximating Al_2O_x than earlier in the experiment.

The resonant frequency shifts also indicated the slowest rate of growth of product in 6061 which is consistent with the earlier thickness analysis. Both 2024 and 7075 show fairly rapidly growing product layers with quite high loss tangents. The growth rates can be distinguished, however, with that on 2024 being about 10% higher than that for 7075 under these exposure conditions.

4.2.6 High temperature alloys

An alloyed Ti sample was exposed to a heated saline environment as an initial test. While this test clearly does not mimic the actual environment an engine part would be subjected to, it can help establish a detectability limit for the analysis. The primary growth will probably be a contaminated oxide, which should be detectable as in the aluminum alloys, but layer growth may be slower. Before and after exposure contour maps are shown in Fig. 6.

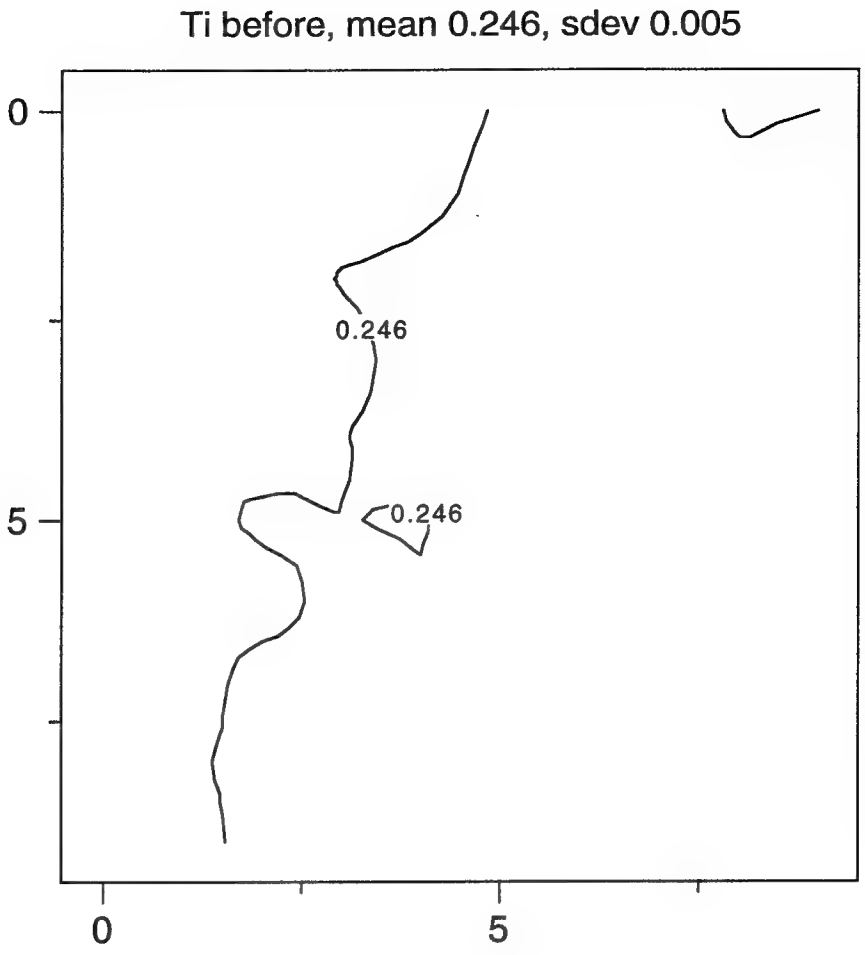
Ti before, mean 0.246, sdev 0.005
0
5
0.246
0.246
0
5

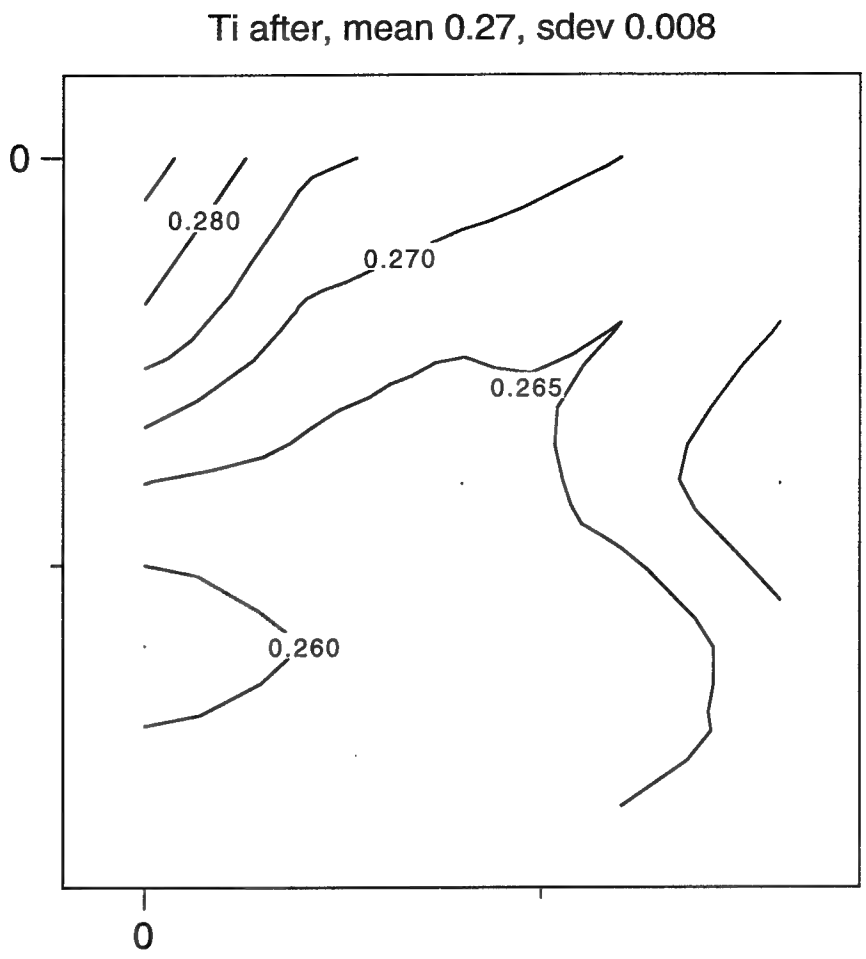

Figure 6. *Plot of a high temperature Ti sample before and after heated saline exposure. While more subtle than some of the other samples, the change in surface resistance is distinct and statistically significant.*

While more subtle, the changes here were detectable and were not visible with the unaided eye. The main purpose of this experiment was to confirm detectability in another important materials family.

4.3 Measurements as a function of other variables: Al alloys with anti-corrosion coatings

The results discussed earlier illustrated the ability of the technique to detect corrosion early and to provide some information about the corrosion products. In the set of samples discussed in this section, the coupons were coated with a corrosion inhibitor and measured before and after a 24 hour salt fog exposure. The goals were to see if the inhibitor could be detected, to look at the corrosion products and to compare them to those on the uncoated samples from the first batch. The particular inhibitor used is being developed separately (outside of this program) by a department at Sandia National Laboratories and is a precipitation film containing Al-Li hydroxide-carbonate-hydrate, an inhibitor which avoids the environmental problems of hexachromates.

A table of surface resistances (in ohms) is shown below for three alloys illustrating the measurements. All values are averages over at least a 2 cm x 2 cm box on each sample with a rastering step size of 2 mm. The exposed sample surfaces measured were all on the leeward side of the salt fog source.

Alloy	Uncoated No exposure	Coated No exposure	Uncoated 24 hr salt fog	Coated 24 hr salt fog
2024	0.248	0.275		0.280
6061	0.222	0.233	0.266	0.245
7075	0.258	0.291	0.376	0.305

In all cases, the coating caused an elevation in measured surface resistance. This is simply because a lossy dielectric film has been added. Part of the rf power is dissipated in the coating, resulting in a higher effective surface resistance. It is important to note, however, that the change in resonant frequency per unit change in surface resistance is much higher for the coating than for the first corrosion products. This indicates that the loss tangent of the coating is much lower than that of the corrosion products and that the effects can possibly be separated. It is thus possible that this technique could be

used as a quality control tool to check if the coating had been applied properly. To completely evaluate that application, more detailed dielectric analysis of the coating would have to be performed.

The corrosion products themselves are quite interesting. The fractional increase in surface resistance after salt fog exposure was much lower for the coated samples than for the uncoated. For 6061, there was a 20% increase in surface resistance without a coating, but only a 5% increase when coated. For 7075, there was a 46% increase in surface resistance without a coating, but a 5% increase with the coating. This is a fairly dramatic difference and is itself interesting. Since the resonant frequency shifts scaled in roughly the same proportion as did surface resistance, it is likely that the predominant cause of the smaller increase is that the corrosion product is not as thick on the coated samples. This, in turn, suggests that the composition of the corrosion products did not change significantly when the coating was used. In all cases, the corrosion was not optically evident other than through slight color shifts(as with the first batch).

To better illustrate the effects, contour maps of all four instances of the 7075 alloy are shown in Fig. 7. The uncoated maps are taken from the first period report for comparison. It is interesting to note that there is not only less corrosion on the coated vs. the uncoated sample, but that the standard deviation is lower as well. It was noted previously that the corrosion may tend to proceed from certain hot spots. The important points are that the corrosion was detected early, quantified to some degree , and some evidence was established that the corrosion stoichiometry did not change significantly with the presence of the coating.

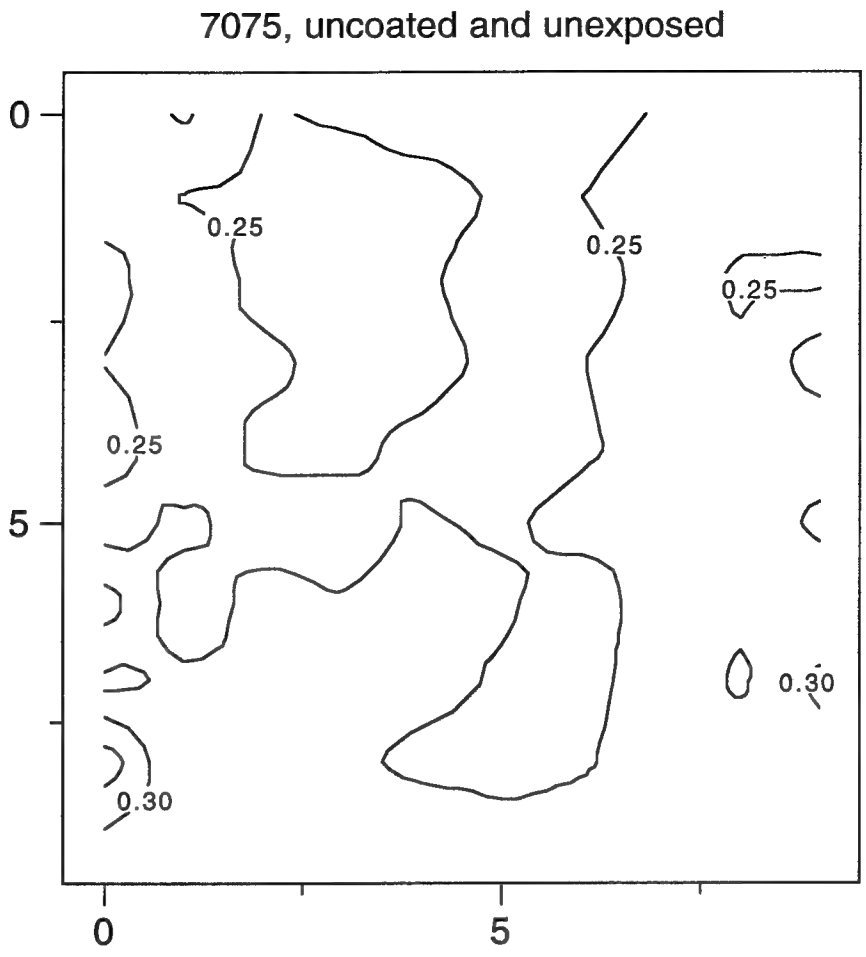

(A)

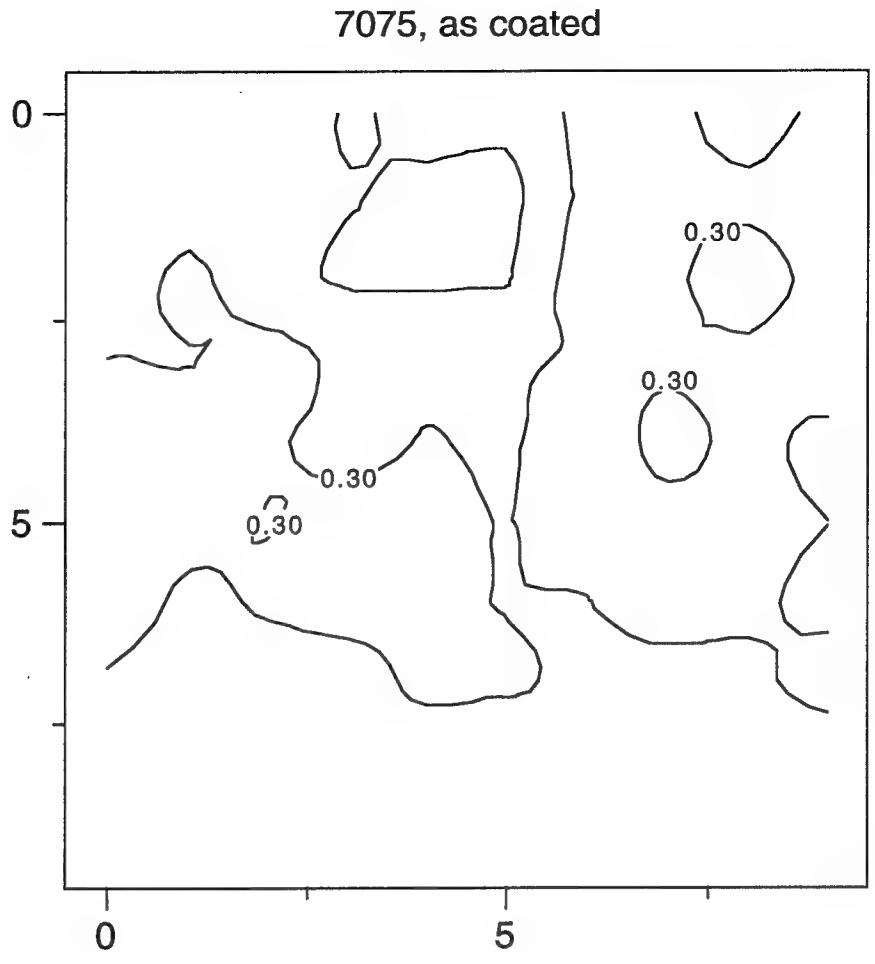

(B)

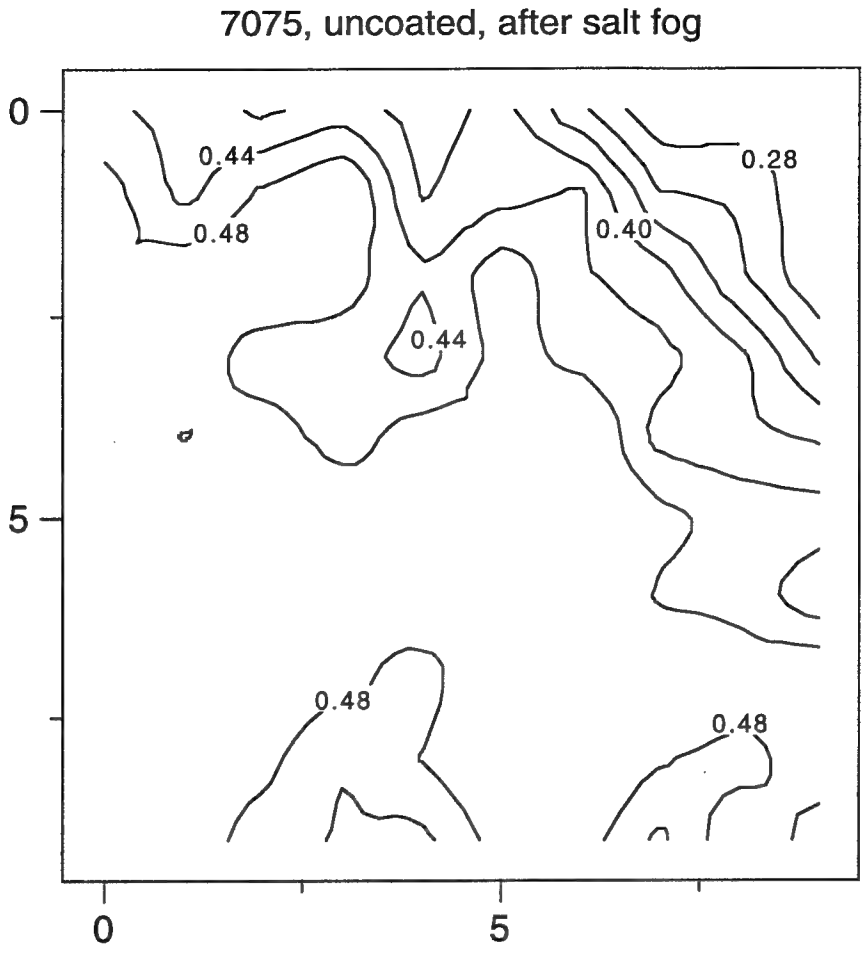

(C)

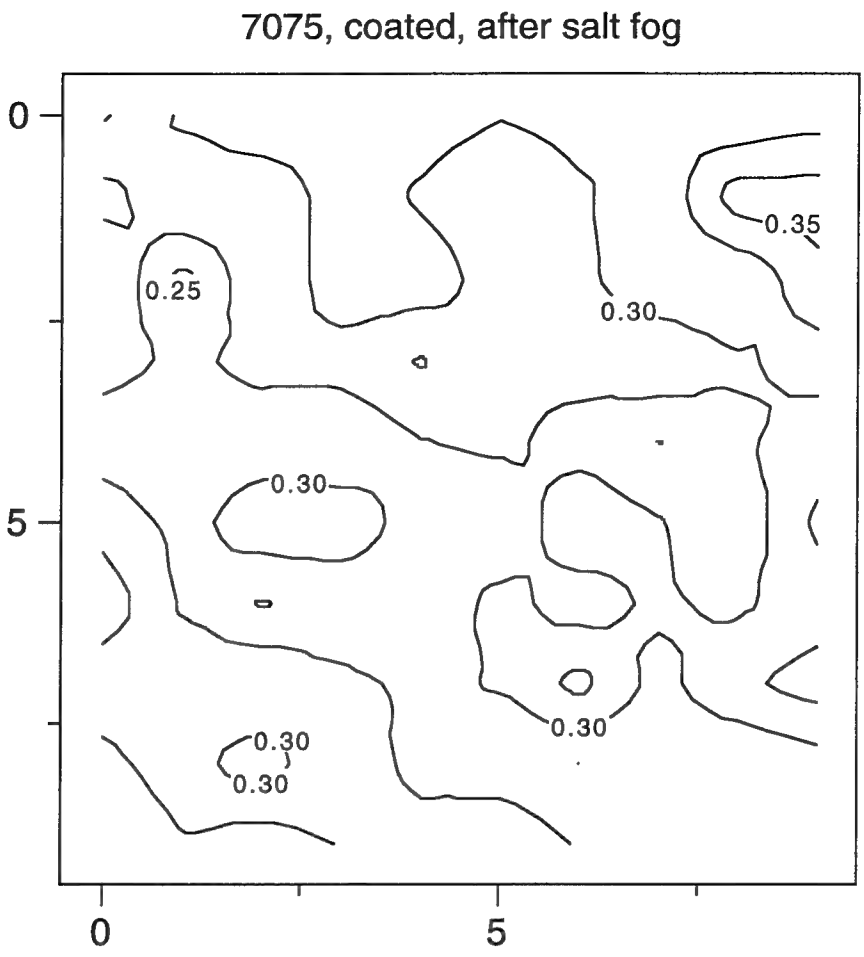

(D)

Figure 7. *Surface resistance contour maps (labels in ohms) of 7075 coupons. The lateral scale in all cases is 2 mm/div. The images are (a) uncoated and unexposed, (b) coated and unexposed, (c) uncoated and exposed to salt fog, (d) coated and exposed to salt fog. The exposed measurements were made on the leeward side of the samples.*

References

[1] G. D. Boyd and J. P. Gordon, Bell Sys. Tech. Jour. **40**, 489 (1961).

[2] J. S. Martens, V. M. Hietala, D. S. Ginley, T. E. Zipperian and G. K. G. Hohenwarter, Appl. Phys. Lett. **58**, 2543 (1991).

[3] R. F. Harrington, Time harmonic electromagnetic fields, McGraw-Hill, New York, 1961, Chp. 7.

[4] J. S. Martens, S. M. Garrison, and S. A. Sachtjen, Solid State Tech. **37**, no. 12, 51 (1994).

[5] J. S. Martens, D. S. Ginley, and N. R. Sorensen, J. Electrochem. Soc. **139**, 2886 (1992).

5 Findings and conclusions:

Section 4 has described in some detail the results of experiments on detectability and analysis for corrosion products on various aluminum alloys, steel and one higher temperature material. In all cases, the mm-wave technique known as surface resistance analysis showed reasonably high sensitivity to the corrosion products (better than optical, often as good as microscopic or weight change analysis) and was able to extract information such as product thickness, relative purity and dependence of purity on test conditions. To summarize:

- Al alloys. Detected corrosion (in a statistically significant fashion) before optically visible. Differentiated between growth rates on different alloys and gave an indication of relative purity of the product layers. Detection and analysis of layers at 100 nm. Detected differences in growth rates and composition shifts in 3-alloy matrix experiment.

- Steel. An easy detection problem but was able to give a product thickness estimate and a growth curve.

- Ti. Only one higher temperature material was tested, but corrosion was detectable on this material as well.

- Rivet holes. Stress corrosion cracks were detected on an Al alloy near hole sites; detectability limit somewhere near 100 μm.

- Under paint. Corrosion was detected under a variety of paints which is critical for field applications.

-Pretreatments. The presence of a pretreatment was detectable prior to exposure (which may be useful for some QC applications). Was able to confirm the success at reducing product growth by at least a factor of 3. This measurement could be independently useful for pretreatment research.

It would seem that the detectability limits are sufficiently low that the instrument would provide added services to an inspector on a variety of materials and structures. On simple structures, a large amount of information about the corrosion products can be extracted. This could be useful for studying new nucleation models on different materials or structures, the study and evaluation of new pretreatments, or the study of the effects of a different test environment. On the detectability side, the two most important experiments done in this program are probably centered around the rivet holes scanning and the imaging underneath paint. Corrosion-related cracking is of considerable economic importance and has proved difficult to detect in some near-surface condition such as the rivet holes. The preliminary results here are somewhat encouraging in that these subsurface distortions are mm-wave detectable. Considerable additional work is, of course, required to determine if this is a useful and field applicable test methodology but it does appear interesting.

The detection of corrosion beneath paint is of significant practical importance. Clearly one does not want to remove paint from an aircraft in service to check for incipient corrosion if at all possible. If surface resistance analysis is sufficiently useful in detecting early corrosion, the repainting schedule could be lengthened or put on a detection basis. A reduction in painting frequency would have enormous direct maintenance savings plus reduce some pressure from volatile organics controls.

The results suggest that surface resistance analysis based on a mm-wave resonant structure combines some significant detection advantages with the ability to extract some interesting analytical information. Work remains to be done in firmly quantifying the detection limits and the field applicability.

6 Implications

The mm-wave measurement technique discussed here seems to be a powerful tool for the detection and analysis of corrosion products. Since a desirable goal is a field usable tool to speed/enhance the repair and maintenance of airframes, there are several steps that should be performed next:

-Confirm detection performance on more realistic structures particularly as related to rivet hole cracking. A matrix study of such holes and exposure conditions would provide valuable information.

-Begin designing a field usable instrument. The primary considerations will be in vibration control. It will be important to assess any changes in repeatability and sensitivity in a more physically demanding environment.

If these challenges are successfully handled, a valuable tool to help the maintenance of military and commercial airframes is possible. Because of the enormous economic problem that corrosion repair/maintenance represents, the impact of such a tool could be substantial. A phase II SBIR proposal has been generated to work towards this goal of a field usable mm-wave NDE tool. We believe such a tool is a natural extension of our product line in the surface resistance analysis area and, if successful, would be of substantial benefit to the government and commercially.